

Development of a hybrid PIC/DSMC Code

IEPC-2005-71

*Presented at the 29th International Electric Propulsion Conference, Princeton University,
October 31 – November 4, 2005*

Monika Auweter-Kurtz^a, Markus Fertig^b, Dejan Petkow^c and Torsten Stindl^d
Institut für Raumfahrtsysteme, Universität Stuttgart, D-70550 Stuttgart, Germany

Martin Quandt^e and Claus-Dieter Munz^f
Institut für Aerodynamik und Gasdynamik, Universität Stuttgart, D-70550 Stuttgart, Germany

Panos Adamidis^g, Michael Resch^h and Sabine Rollerⁱ
Höchstleistungsrechenzentrum Stuttgart, D-70550 Stuttgart, Germany

Danilo D'Andrea^j and Rudolf Schneider^k
*Institut für Hochleistungsimpuls und Mikrowellentechnik, Forschungszentrum Karlsruhe,
D-76133 Karlsruhe, Germany*

In order to model rarefied plasma flows under conditions where continuum assumptions fail, a cooperation between IRS (Institute of Space Systems, University of Stuttgart), IAG (Institute for Aerodynamics and Gas Dynamics, University of Stuttgart), HLRS (High Performance Computing Center Stuttgart) and IHM (Institute for Pulsed Power and Microwave Technology, Research Center Karlsruhe) has been formed. Within the project "Modeling and Simulation on High Performance Computers", which is funded by the Landesstiftung Baden-Württemberg, a scheme for solution of the Boltzmann equation for rarefied, non-continuum plasma flows is under development making use of well known approaches from PIC (Particle in Cell) and DSMC (Direct Simulation Monte Carlo). The modeling will be explained in some detail and first results will be presented.

^aProfessor, Head of Department, Raumtransporttechnologie, auweter@irs.uni-stuttgart.de

^bHead of Plasma Modelling and Simulation Group, Raumtransporttechnologie, fertig@irs.uni-stuttgart.de

^cScientist, Raumtransporttechnologie, petkow@irs.uni-stuttgart.de

^dScientist, Raumtransporttechnologie, stindl@irs.uni-stuttgart.de

^eScientist, quandt@iag.uni-stuttgart.de

^fProfessor, munz@iag.uni-stuttgart.de

^gScientist, Department for Parallel Computing, adamidis@hlrs.de

^hProfessor, Director HLRS, resch@hlrs.de

ⁱScientist, Department for Applications, Models and Tools, roller@hlrs.de

^jScientist, danilo.dandrea@ihm.fzk.de

^kSenior Fellow, rudolf.schneider@ihm.fzk.de

Nomenclature

\vec{B}	magnetic induction
\vec{c}	molecular velocity
d	diameter
\vec{E}	electric field
F	external force
f	velocity distribution function
g	relative velocity
\vec{j}	current density
m	particle mass
n	particle density
p	pressure
T	temperature
t	time
\vec{V}	thermal velocity
\vec{v}	mass average velocity
\vec{x}	coordinate

Greek Symbols

ϵ_0	electric permittivity
μ_0	magnetic permeability
ω	viscosity coefficient
ρ	charge density
ρ	density
σ	collision cross section
Ω	solid angle

Constants

c	speed of light
k	Boltzmann's constant

Subscripts

$coll$	Collisions
i, j	species indices
r	reduced
ref	reference
T	total

Abbreviations

DSMC	Direct Simulation Monte Carlo
ESA	European Space Agency
HLRS	Höchstleistungsrechenzentrum Stuttgart
IAG	Institut für Aerodynamik und Gasdynamik
IHM	Institut für Hochleistungsimpuls und Mikrowellentechnik
IMPD	instationary magnetoplasma dynamic
IRS	Institut für Raumfahrtsysteme
PIC	Particle in Cell
PPT	Pulsed Plasma Thruster

I. Introduction

WHILE PIC (Particle in Cell) methods allow the modeling of charged particle movement within electromagnetic fields, they do not usually take into account interactions between particles, i.e. collisions leading to energy and momentum exchange as well as to chemical reactions. Since these interactions can play an important role for the thrust and losses of electric propulsion systems, it is necessary to model them as well, using e.g. DSMC (Direct Simulation Monte Carlo) techniques. A cooperation between IRS (Institute of Space Systems, University of Stuttgart), IAG (Institute for Aerodynamics and Gas Dynamics, University of Stuttgart), HLRS (High Performance Computing Center Stuttgart) and IHM (Institute for Pulsed Power and Microwave Technology, Research Center Karlsruhe) has been formed to develop a hybrid PIC/DSMC scheme.

The main application for this scheme is the modeling of an instationary magnetoplasmadynamic (IMPD) thruster, also known as pulsed plasma thruster (PPT). Within the small satellite program of the IRS, a lunar satellite is under development. The satellite will be equipped with two electric propulsion systems. The main propulsion system will consist of a cluster of IMPD thrusters. The duration of a single pulse is of the order of $8 \mu\text{s}$. The current of about 30 kA allows an acceleration of the propellant mass bit leading to exhaust velocities of about 12 km/s, i.e. a specific impulse of approximately 1200 s .¹ Due to the instationary operation and the degree of rarefaction, no continuous partition function of the propelling plasma is to be expected.

A second application is the modeling of a combined electrodynamic tether/ electric propulsion (CETEP) system proposed by ESA.² The thrust generated by an electrodynamic tether is limited by its current collection ability. The PMG (Plasma Motor Generator) aboard the TSS-1R (Tethered Satellite System), for example, was able to reach 0.3 A in flight under the best ionospheric conditions.³ For a coupled system, the tether links an ion thruster and its neutralizer. The electrons generated in the ion thruster are driven through the tether and released by the neutralizer. Thereby, the tether current is only limited by the number of electrons produced by the ion engine, resulting in a possible current of the order of 2-3 A (depending on the ion thruster used) and therefore a higher tether thrust, which is additionally amended by the thrust of the ion engine itself.

In order to model the physics, the PIC scheme developed by IHM^{4,5} will be extended by models for intraspecies charged particle collisions and intermolecular reactions. Within the PIC code, the Vlasov-Maxwell equations are solved in order to describe the interaction between charged particles and electromagnetic fields. To model the exchange of momentum and energy as well as chemical reactions without consideration of Lorentz forces, a DSMC method based on the "LasVegas" code developed at IRS⁶ is used. A newly developed Fokker-Planck solver using PIC techniques is used to model collision relaxation of electrons in velocity space. The integration of these three models is expected to allow for an accurate prediction of the thrust of electric space propulsion systems operating far from continuum. Additionally, the necessity of a three dimensional and time accurate description and complex geometries requires optimization and parallelization of the code in order to efficiently use high performance computers.

In Section II, a description of the problem – finding a general solution to the Boltzmann equation – and the simplifications used are given. In Sections III, IV, and V, an overview of the methods used to model the various parts of the Boltzmann equation is given. In Section VI, conceptual aspects are discussed to manage the interplay of the three different models. First results are presented in Section VII and, finally, a short summary and an outlook are given in Section VIII.

II. Boltzmann Equation

From the microscopic point of view, a particle without internal degrees of freedom can be characterized by its mass and velocity. Combining all particles with equal mass m_i within a volume element $dx_1 dx_2 dx_3$ defines a phase space distribution function

$$f_i(\vec{x}, \vec{c}_i, t), \quad (1)$$

where \vec{c}_i is the particle velocity and t is the time. In many cases, mean macroscopic gas properties are necessary, which can be found by evaluation of

$$\rho = m \int f d\vec{c} \quad \text{for the density,} \quad (2)$$

$$\vec{v} = \frac{1}{n} \int \vec{c} f d\vec{c} \quad \text{for the velocity,} \quad (3)$$

$$T = \frac{m}{3nk} \int V^2 f d\vec{V} \quad \text{for the temperature and} \quad (4)$$

$$\bar{p} = m \int \vec{V} \vec{V}^T f d\vec{V} \quad \text{for the pressure,} \quad (5)$$

where the thermal velocity \vec{V}_i is defined by

$$\vec{V}_i = \vec{c}_i - \vec{v}, \quad (6)$$

and n denotes the number density, which is given by $n = \int f d\vec{c}$. The most general equation describing the change of the distribution function is the Boltzmann equation

$$\frac{\partial f_i}{\partial t} + \vec{c}_i \cdot \nabla_x f_i + \frac{\vec{F}_i}{m_i} \cdot \nabla_c f_i = \left(\frac{\delta f_i}{\delta t} \right)_{Coll}, \quad (7)$$

which describes the change of the distribution function in time and phase space as a result of external forces and particle collisions. The term on the right-hand side of Eq. (7) represents the Boltzmann collision integral⁷

$$\left(\frac{\delta f_i}{\delta t} \right)_{Coll} = \sum_j \int g(\vec{c}_i, \vec{c}_j) \sigma_{ij}(g) \left[f'_i(\vec{c}'_i) f'_j(\vec{c}'_j) - f_i(\vec{c}_i) f_j(\vec{c}_j) \right] d\Omega d\vec{c}_j, \quad (8)$$

which reflects the rate of change with respect to time of f_i due to collisions. Here, the index j runs over all “scattering” populations, $\vec{g} = \vec{c}_i - \vec{c}_j$ is the relative velocity, $\sigma_{ij}(g)$ is the differential scattering cross section between the particles of the species i and j and the element of solid angle $d\Omega$ is given by $d\Omega = \sin \theta d\theta d\phi$. Moreover, the prime refers to the value of a quantity after a collision and unprimed denotes the values before the collision. From the mathematical point of view, the Boltzmann equation is a very complicated integro-differential equation which can be used to determine the velocity distribution function. Up to now, a general solution of the Boltzmann equation to describe macroscopic problems is not possible. Therefore, several simplifications are necessary to compute solutions for the Boltzmann equation. In the case of highly non-neutral plasmas, the right-hand side of the Boltzmann equation (7) can be neglected. Then, the collective behavior of such an electrically non-neutral ensemble of charged particles is described by the Vlasov and Maxwell equations.⁴ The corresponding numerical approach is known as the Maxwell-Lorentz model, which is based on Particle-in-Cell techniques. A very brief review of this model is given in section III. However, in order to model the physics of a PPT, collisions between particles of the same species as well as between different species have to be taken into account. An appropriate, lowest order approximation of the collision integral (8) leads to the Fokker-Planck model.⁸ This approach is suitable for modeling intraspecies charged particle collisions and will be introduced in Section IV. A further approximation of the collision integral that allows the inclusion of interspecies reactions is presented in Section V. Therein, the underlying DSMC method is applied to model ionization and recombination processes.

III. Maxwell's Equations

According to the law of dynamics for charged particles, the external force \vec{F}_i in equation (7) is determined by the Lorentz force and depends on the velocity \vec{c}_i , the electric field \vec{E} , and the magnetic induction \vec{B} :

$$\vec{F}_i = q[\vec{E}(\vec{x}, t) + \vec{c}_i \times \vec{B}(\vec{x}, t)]. \quad (9)$$

With the Lorentz force for charged particles (9), the Boltzmann equation (7) can be written in the collisionless kinetic formulation for the distribution function f_i of the charged particles, the so called Vlasov equation

$$\frac{\partial f_i}{\partial t} + \vec{c}_i \cdot \nabla_x f_i + \frac{q_i}{m_i} (\vec{E}(\vec{x}, t) + \vec{c}_i \times \vec{B}(\vec{x}, t)) \cdot \nabla_c f_i = 0. \quad (10)$$

In the terminology of hyperbolic partial differential equations, the general solution of (10) is given by its characteristics, the Lorentz equations

$$\frac{d\vec{x}_i}{dt} = \vec{c}_i, \quad (11)$$

$$\frac{d\vec{p}_{m,i}}{dt} = \vec{F}_i. \quad (12)$$

The relativistic momentum is given by $\vec{p}_{m,i} = m_i \gamma c_i$ with the Lorentz factor $\gamma^2 = 1 + (\vec{p}_{m,i}/(m_i c_L))^2$ where c_L denotes the speed of light.

The difficulties in solving the Lorentz equations arise from the fact that the electric field \vec{E} and the magnetic induction \vec{B} are not given explicitly. They have to be calculated at each time step in a self-consistent manner⁹ from the full set of Maxwells equations

$$\frac{\partial \vec{E}}{\partial t} - c^2 \nabla \times \vec{B} = -\vec{j}, \quad \text{Ampère's law,} \quad (13)$$

$$\frac{\partial \vec{B}}{\partial t} + \nabla \times \vec{E} = 0, \quad \text{Faraday's law of induction,} \quad (14)$$

$$\nabla \cdot \vec{E} = \frac{\rho}{\epsilon_0}, \quad \text{Gauss' law,} \quad (15)$$

$$\nabla \cdot \vec{B} = 0, \quad \text{absence of magnetic monopoles,} \quad (16)$$

where the electric permittivity ϵ_0 and magnetic permeability μ_0 are related to the speed of light c_L according to $\epsilon_0 \mu_0 c_L^2 = 1$. For given charge and current densities ρ and \vec{j} , the Maxwell equations describes the temporal and spatial evolution of the electric field \vec{E} and the magnetic induction \vec{B} . With an integration over the entire range of momentum $\vec{p}_{m,i}$, the self consistent parts of the charge and current density ρ , \vec{j} are obtained from¹⁰

$$\rho = \sum_i q_i \int f_i(\vec{x}, \vec{p}, t) d^3 p, \quad (17)$$

$$\vec{j} = \sum_i q_i \int \vec{c}_i f_i(\vec{x}, \vec{p}, t) d^3 p. \quad (18)$$

Up to now the description is exact in the sense that no numerical approximations are made.

For the numerical realization of the Maxwell-Lorentz system, the Particle-In-Cell method is applied.¹¹ In the discrete case, the charge and current density can be obtained from

$$\rho^* = \sum_i q_i \delta[\vec{x} - \vec{x}_i] \quad (19)$$

$$\vec{j}^* = \sum_i q_i \vec{c}_i \delta[\vec{x} - \vec{x}_i], \quad (20)$$

where δ denotes the usual Dirac function. For each grid node, all particles in the surrounded cells are considered. In order to determine the contribution of the particles, shape-functions are used to calculate ρ and \vec{j} at the grid nodes. With these charge and current densities the new electromagnetic fields are computed

at these nodes and then interpolated to the local particle positions. To get these field values, the Maxwell equations have to be solved at each time step.

A direct consequence of the charge conservation equation

$$\frac{\partial \rho}{\partial t} + \nabla \cdot \vec{j} = 0. \quad (21)$$

and of the fact the divergence of the curl for any differentiable vector field being zero is that the divergence constraints (16) and (15) are satisfied for all times, if the initial values satisfy these relations. In this case, it would be sufficient to solve the hyperbolic evolution equations (13) and (14) only.

Unfortunately, in the simulation numerical errors may occur: The divergence of a curl may be zero up to some error terms only and interpolation errors in the particle treatment may arise. This leads to small errors being introduced at each time step. If only the hyperbolic evolution equations are numerically solved, then these errors may increase and strongly falsify the solution. For a self-consistent movement of charged particles, the Gauss law (15) and the statement about the absence of magnetic monopoles (16) have to be coupled with Ampère's and Faraday's law. In the Generalised Langrange Multiplier (GLM) approach two additional variables $\Phi(\vec{x}, t)$ and $\Psi(\vec{x}, t)$ are introduced into the Maxwell equations to couple the evolution equations for the electromagnetic fields (13) and (14) with their elliptical constraints (15) and (16), respectively. The coupling terms may be chosen such that a purely hyperbolic system can be formed.¹² If the errors are Zero, then it coincides with the original Maxwell equations. The Purely Hyperbolic Maxwell (PHM) equations system reads as

$$\frac{\partial \vec{E}}{\partial t} - c^2 \nabla \times \vec{B} + \chi c^2 \nabla \Phi = -\frac{\vec{j}}{\epsilon_0}, \quad (22)$$

$$\frac{\partial \vec{B}}{\partial t} + \nabla \times \vec{E} + \gamma \nabla \Psi = 0, \quad (23)$$

$$\nabla \cdot \vec{E} + \frac{1}{\chi} \frac{\partial \Phi}{\partial t} = \frac{\rho}{\epsilon_0}, \quad (24)$$

$$\nabla \cdot \vec{B} + \frac{1}{\gamma c^2} \frac{\partial \Psi}{\partial t} = 0, \quad (25)$$

where the dimensionless positive parameters χ and γ represent the transportation coefficients for the local errors Φ and Ψ . These new variables $\Phi(\vec{x}, t)$ and $\Psi(\vec{x}, t)$ define two additional degrees of freedom and couple the divergence conditions (15), (16) to the evolution equation (13), (14).

This correction technique ensures that the divergence errors arising from the *div curl* as well as from the charge conservation violation within an electromagnetic PIC computation cannot increase and falsify the numerical simulation results. A decisive advantage of the proposed FV approach is that the explicit numerical methods used for the Maxwell equations in the time domain can be combined with a hyperbolic divergence correction in a straightforward manner, yielding a very efficient and highly flexible Maxwell solver module for PIC applications on unstructured grids and for parallel computing.

IV. A Diffusion Model for Charged Particles Interaction in PIC Simulation

In the following, we consider a plasma where electron-electron collisions – abbreviated by (e,e) – play an important role. We assume that the electron density is of the order of 10^{18} m^{-3} , which means that the (e,e)-collision frequency exceeds the one of electron-neutral collisions. It is obvious that in such plasmas the shape of the electron energy distribution function (EEDF) is mainly determined by the (e,e)-interactions. In the case where the energy input into the plasma goes primarily into the thermal part of the EEDF, the high-energy tail is mainly populated by energy up-scattering caused by (e,e)-collisions. Furthermore, these collisions always drive the EEDF towards a Maxwellian distribution. However, in this situation a competition with inelastic electron-neutral reactions occurs, which depletes the high-energy tail. Another competition may be relevant in bounded plasmas, since high-energy electrons can escape to the walls. Energetic considerations

indicate that the high-energy tail controls reactions like atomic excitation and ionization, and to some extent the plasma chemistry. Clearly, since the EEDF determines many properties of the plasma, it is essential to model (e,e)-collisions as realistic as possible. In the following, we describe the formulation that allows to include (e,e)-collisions into a PIC framework in a natural way.

A. Governing Equations

A well-established and for our purposes suitable mathematical model for (e,e)-collisions is given by the Fokker-Planck (FP) equation

$$\left(\frac{\delta f}{\delta t}\right)_{Coll} = -\frac{\partial}{\partial c_j} [\mathcal{F}_j f] + \frac{1}{2} \frac{\partial^2}{\partial c_j \partial c_k} [\mathcal{D}_{jk} f]. \quad (26)$$

This model describes the evolution of the electron distribution function $f = f_e(\vec{x}, \vec{c}, t)$ as a result of small-angle scattering of Coulomb point particles, and represents the lowest order approximation of the Boltzmann collision integral.^{8,13,14} The key quantities to determine the coefficients of dynamical friction $\mathcal{F}_j(\vec{x}, \vec{c}, t) \sim \partial \mathcal{H} / \partial c_j$ and diffusion $\mathcal{D}_{jk}(\vec{x}, \vec{c}, t) \sim \partial^2 \mathcal{G} / \partial c_j \partial c_k$ are the Rosenbluth potentials¹⁵ given by

$$\mathcal{H}(\vec{x}, \vec{c}, t) = 2 \int_{-\infty}^{\infty} \frac{f(\vec{x}, \vec{w}, t)}{|\vec{g}|} d^3 w \quad (27)$$

and

$$\mathcal{G}(\vec{x}, \vec{c}, t) = \int_{-\infty}^{\infty} |\vec{g}| f(\vec{x}, \vec{w}, t) d^3 w, \quad (28)$$

where $\vec{g} = \vec{c} - \vec{w}$ is the difference between the velocity of the scattered-off electrons and the velocity of the electrons that serve as scatterer. Clearly, the friction force \vec{F} and the diffusion tensor \mathbf{D} themselves depend on the velocity \vec{c} , hence, the FP model generally is a complicated non-linear problem that has to be solved numerically in an appropriate – namely, self-consistent – manner. Note that the appearance of the FP equation reveals that the (e,e)-collisions are modeled as a diffusion process that describes the short-time behavior of the considered system.^{16,17}

The FP equation (26) for the evolution of f is equivalent to the stochastic differential equation (SDE) in the Itô sense^{16,18}

$$d\vec{C}(t) = \vec{F}(\vec{C}, t) dt + \mathbf{S}(\vec{C}, t) d\vec{W}(t), \quad (29)$$

where $\vec{W}(t)$ represents the three-dimensional Wiener process and the matrix $\mathbf{S} \in \mathcal{R}^{3 \times 3}$ is related to the diffusion matrix according to $\mathbf{D} = \mathbf{S} \mathbf{S}^T$. As indicated, both quantities \vec{F} and \mathbf{S} now depend on the stochastic variable $\vec{C} = \vec{C}(t)$, which will be identified later as the velocity of a single (macro) electron. Hence, the use of the Langevin-type SDE (29) fits in a remarkable way into the standard PIC approach,⁴ which is one basic concept of the present code development.

It is well known that the assumption of an isotropic but non-Maxwellian velocity distribution of the scatterer implies an enormous reduction of the problem since the diffusion and friction coefficients can be written in terms of one-dimensional quadratures.^{15,19,20} In order to be free of any model (assumption), we have to start from the Rosenbluth potentials (27) and (28) and apply Fourier transformation techniques to compute the integrals in velocity space. After some standard manipulations,²¹ we obtain the results

$$\mathcal{H}(\vec{c}) = 8 \pi F^{-1} \left\{ \frac{\hat{f}(\vec{k})}{k^2} \right\} \quad (30)$$

and

$$\mathcal{G}(\vec{c}) = -8 \pi F^{-1} \left\{ \frac{\hat{f}(\vec{k})}{k^4} \right\}, \quad (31)$$

where the identity $\nabla_{\vec{c}}^2 g = 2/g$ has been used to obtain the second relation and F^{-1} denotes the inverse Fourier transformation of the arguments in the braces. Clearly, the arguments of (30) reveal the convolution character of expression (27), which means that we get in \vec{k} -space the product of the Fourier transform $\hat{f}(\vec{k}) = (2\pi)^{-3/2} \int_{-\infty}^{\infty} d^3c e^{-i\vec{k}\cdot\vec{c}} f(\vec{c})$ and $1/k^2$, which is the Fourier transformation of the ‘‘Coulomb potential’’ $1/g$. In essence, the main advantage of the Fourier approach is that we obtain a first principle, fully self-consistent determination of the deterministic friction and stochastic diffusion arising in (26) and (29) since no specific model assumptions are necessary to compute the Rosenbluth potentials.

B. Numerical Framework

For the sake of clearness, we consider a single spatial grid cell, in which a sufficiently large number of particles is located, and assume that a computational Cartesian mesh in velocity space is associated with this local grid zone.

Assignment. From the actual location of the plasma particles in mesh-free velocity space, the distribution function $f(\vec{c})$ is constructed on the Cartesian velocity mesh by applying linear assignment techniques similar to those discussed in.¹¹

Rosenbluth Solver. Afterwards, Fast Fourier Transformation (FFT) methods^{22,23} are applied to compute the Fourier transform $\hat{f}(\vec{k})$ of the distribution function $f(\vec{c})$ and the subsequent convolution of $\hat{f}(\vec{k})$ with the transform of $1/g$. Finally, an inverse transformation yields the grid-based Rosenbluth potentials (30) and (31), from which the friction force and the diffusion matrix can be determined. In order to avoid ‘‘computational noise’’, often associated with differentiation, it seems to be advantageous to directly compute the derivatives of the potentials in the FFT context.

Interpolation. The ‘‘Langevin forces’’, which are the deterministic friction and the stochastic diffusion, have to be computed at the position of each particle in grid-free velocity space. For that, linear interpolation techniques are used, which can be found, for instance, in reference.¹¹

Langevin Solver. Under the action of the velocity-dependent Langevin forces, each particle is moved in velocity space according to the SDE (29), where appropriate numerical methods are required. For our purposes, we use strong approximations¹⁸ of equation (29). For instance, the Euler scheme²⁴

$$\vec{C}^{n+1} = \vec{C}^n + \vec{F}(\vec{C}^n, t^n) \Delta t + \sum_{i=1}^3 \vec{\sigma}_i(\vec{C}^n, t^n) \Delta W_n^i \quad (32)$$

is applied, which converges strongly with order $\gamma = 1/2$. In the latter equation, $\vec{\sigma}_i = \mathbf{S} \cdot \vec{e}_i$, with the unit vector \vec{e}_i , and the Wiener increment ΔW_n^i is defined according to $\Delta W_n^i = \sqrt{\Delta t} \eta_i$, where Δt is the time step size and $\eta_i \sim \mathcal{N}(0, 1)$ denotes a Gaussian distributed random number with mean $\mu = 0$ and variance $\sigma^2 = 1$. Note, that the order of the Euler scheme can easily be improved by adding an additional term of the Itô-Taylor expansion, which leads to an explicit order $\gamma = 1$ scheme proposed by Milstein.²⁴ This step closes the self-consistent determination cycles, which have to be run through at each time step and for each spatial grid cell.

V. Modeling of Short Range Particle Interactions

The losses of a thruster using purely electromagnetic acceleration forces can be estimated considering distribution and density of the neutral particles. Since no assumptions can be made due to very low plasma densities and short pulse durations, every single neutral particle has to be tracked in phase space. Moreover, elastic and inelastic interactions have to be considered in order to obtain a physically reasonable composition of the plasma. This is done by applying a DSMC method, which was developed in the 1960s by Bird and became the standard particle approach for simulations of reactive and non-reactive rarefied gases.²⁵ In such gases, the long range particle interaction can be neglected, thus simplifying the collision modeling to binary collisions. The DSMC method approximates the solution of the full non-linear Boltzmann equation (7) for each species, which is formulated for binary collisions as well.

Considering particle collisions on a microscopic level, one must define the intermolecular potential model in order to find an appropriate approximation for σ_{ij} , which is in general a function of g and the scattering angle χ . The simplest approximation is given by the rigid sphere potential function, see Fig. 1. Here, the potential is ∞ for $r < d$ and 0 for $r > d$, whereas the collision diameter is given by $d = (d_i + d_j)/2$. A collision occurs, when the orthogonal distance between both particles b is smaller than d , as shown in Fig. 1. This model leads to isotropic particle scattering and the total collision cross section

$$\sigma_T = \int_0^{4\pi} \sigma d\Omega = \pi d^2, \quad (33)$$

which does not depend on the relative velocity g . However, this non-realistic scattering law and the missing influence of the relative velocity on σ put the advantage of the easy computable collision mechanics of the HS model into perspective.

The accuracy can be increased by applying the inverse power law potential function which is depicted in Fig. 1. The problem in principle, that arises, is that its total cross section may become infinite. Thus, a clear definition of the collision frequency and mean free path is difficult. One way to address this problem is to use the variable hard sphere (VHS) model. Hereby, the isotropic scattering of the HS model is retained, but the molecular diameter, which is a function of the temperature, is allowed to vary as a function of g .

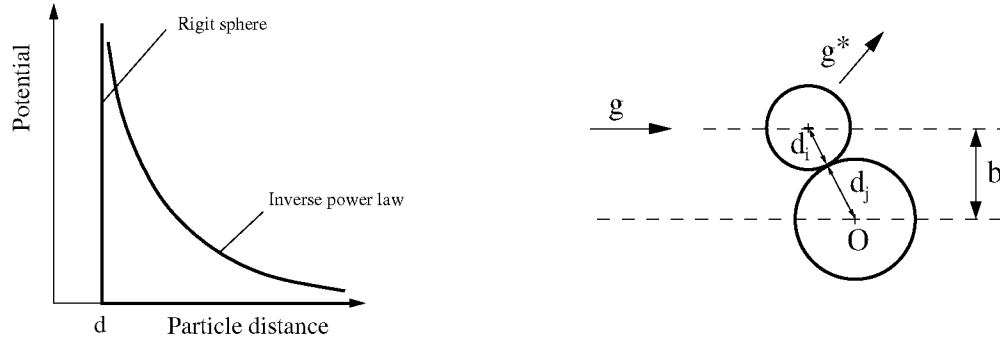


Figure 1: Pictorial representation of interaction potential functions (left) and HS collision mechanic (right)

The effective cross section of real molecules decreases as g increases. The rate of decrease is directly related to the change of viscosity with temperature, namely $\mu \sim T^{\omega+1/2}$. Thus, the resulting collision cross section is

$$\sigma_T(g) = \pi d_{ref}^2 \left(\frac{2(2-\omega)kT_{ref}}{m_r g^2} \right)^\omega, \quad (34)$$

where d_{ref} is a reference diameter at a particular reference temperature T_{ref} , m_r is the reduced mass, k is Boltzmann's constant and ω is the index of the viscosity-temperature power law. For $\omega = 0$, the HS model is obtained, for $\omega = 1/2$, Maxwellian particles are simulated.

The VHS model is relatively simple and yields more accurate results than the HS model. Thus, it became the most common cross section model for DSMC simulations and is used in the particle approach presented here.

Working principle of DSMC

The employed grid structure divides the domain into cells. This is necessary for the splitting of molecular collisions processes in physical space, thus defining the set of potential collision partners for each cell, and for the calculation of macroscopic properties by particle sampling. Similar to PIC, time is advanced by small

steps. The discretization criteria differ from those in PIC. Namely, the cell size and time step have to be much smaller than the molecular mean free path and mean free time in the gas, respectively. This results from the uncoupling of particle motions and collisions.

The evolution of the particle system during one time step Δt proceeds in three steps:

Step 1: After particle localization, reflective gas-surface-interactions are treated by applying one of the following models: The Maxwell model combines specular with diffusive reflection and partial energy accommodation. The Hurlbut-Sherman-Nocilla (HSN) model superimposes the maxwellian reemission with a drift velocity, but does not satisfy detailed balancing. The Cercignani-Lampis (CL) model is the most advanced model which satisfies detailed balancing.

Step 2: Collisions within each cell are calculated in a probabilistic manner. Therefore, the No-Time-Counter (NTC) method is used. Potential collision pairs are sampled by the Natural-Sample-Size (NSS) technique. The random number generator RAN2 is used in order to make the final collision pair selection. For the dissociation reaction the Total Collision Energy (TCE) and Vibrationally-Favored-Dissociation (VFD) models can be applied. For the description of the vibrational modes the Simple Harmonic Oscillator (SHO) as well as the Truncated SHO (TSHO) model can be chosen. The Larsen-Borgnakke model is used in order to distribute the postcollisional energy to inner degrees of freedom. In principle, only particle velocities, inner energies and/or species type may change, whereas spatial positions remain unchanged. In our approach the scale factor describing the number of real particles in a macroparticle is constant and equal for all particles.

Step 3: The particles are advanced using the simple Newtonian mechanics.

The DSMC code used here is based on LasVegas, a DSMC code written by M. Laux during the 1990s at the IRS.⁶ It was developed in order to simulate rarefied gas flows around reentering bodies in earth atmosphere and allows the calculation of relaxation, chemical reactions and gas-surface-interactions of mono- and diatomic gases.

Currently, the chemical models are extended by ionization and the reversal recombination processes, which are necessary for a complete simulation of the performance of an IMPD thruster.

VI. Coupling Concept

An important part of the project is the integration of the four aforementioned building blocks - that are a) the Maxwell solver, b) the Lorentz solver, c) the Fokker-Planck part, and d) the DSMC part - into one code. Part a) is a Finite Volume scheme, based on an (unstructured) computational grid. Parts b - d are particle based systems involving the grid only to determine possibly interacting particles. Therefore, inter- and extrapolation techniques form one main constituent of the coupling. The other are localization procedures to determine the position of a particle within the computational grid. Figure 2 shows the coupled iteration of one timestep.

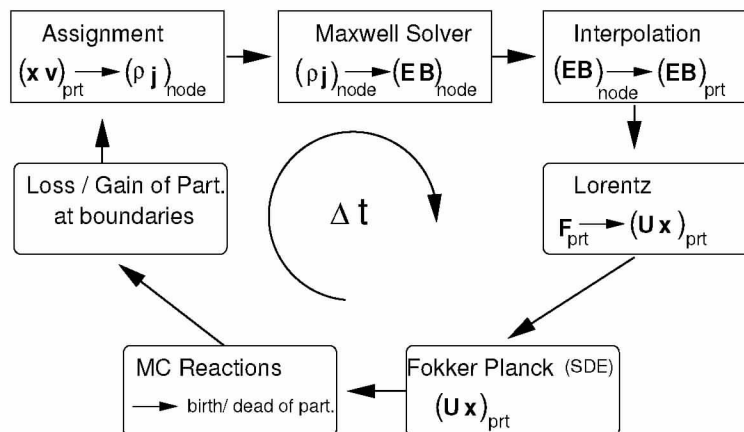


Figure 2: Coupling Circle for the integrated code

Given a particle distribution within the computational domain, the charge and current densities define the electromagnetic eigenfields. Therefore, their values at the particle positions have to be assigned to node or cell values for the Maxwell solver, where they act as source terms. After completing the Maxwell step, the \vec{E} - and \vec{B} -fields are known as cell averages in the Finite Volume context. They have to be evaluated at the particle positions to determine the Lorentz forces acting on the charged particles. Hence, the mean values have to be extrapolated from grid positions to particle positions with the desired order of accuracy. The Lorentz solver then determines the acceleration of the particles. Performing these steps forms the Particle-In-Cell framework.

Next, Fokker-Planck and DSMC steps determine additional velocity changes of the charged as well as uncharged particles due to interactions, i.e. collisions and chemical reactions, as described in Sections IV – V. These steps, as well as the Lorentz solver, act on the same particle distribution, i.e. the distribution at the beginning of the time step, meaning that the different steps do not know about changes introduced by the previous ones. Each step changes the velocity of the particles without actually moving them.

The movement of the particles is done in a separate pushing step. Within this step, the particles have to be localized on the grid to assign to them the grid cell they are in and/or the nearest barycenters or Gaussian integration points. This information is also necessary for the application of correct boundary conditions.

Localization of particles is done in two different ways: If the previous position of the particle is known, the cross-products of the particle velocity vector with particle-to-node vectors are calculated to determine the side face through which the particle has left. Then, the corresponding neighboring cell is checked in the same way. This is an efficient procedure, suitable for vectorization and parallelization.

Newly emitted particles have to be localized differently, since no knowledge from a previous time step is available. In this case, the unstructured computational grid is overlaid by a cartesian-equidistant one. There, the search is done by dividing the position of the particle by the grid size Δx , yielding the correct structured cell for this particle. Then, only the unstructured cells contained in this structured cell have to be checked, until the correct one is found.

The particle push, including the localization of the particles within the grid as well as the application of boundary conditions, is the closing step of each time step, leading to a new particle distribution used in the following time step.

The numerical and implementational requirements of the four building blocks differ strongly, therefore the parallelization strategy is not self-evident. It has been decided to parallelize over the computational domain, i.e. to apply a domain decomposition method. Also, parallelization over the particles was considered. For the Lorentz solver, this would be possible, since all particles move independently. The movement is determined only by electric and magnetic forces acting on them. However, the Fokker-Planck and the DSMC step need information about neighboring particles to determine the interaction probabilities. For this, pairs of nearby particles have to be determined by random processes. Therefore, the particles cannot be considered independent of each other and it has to be guaranteed that these particles remain on the same processor. Thus, a grid based domain decomposition containing not only the cell values but also the information about all particles located in these cells is chosen as parallelization strategy.

In order to reduce the computational time for particle localizations, especially of the newly emitted particles, all geometrical information about the unstructured-structured cell link is calculated in an initialization step prior to the time iteration procedure. Here, mapping matrices of structured grid cells and the contained unstructured cells have to be generated. These matrices are sorted in order to reduce the bandwidth and to obtain long loops for better optimization.

VII. First Results

The different models described in Sections III to VI have been combined into one numerical code and verification tests are being conducted. In the following, first results of these tests are presented.

The PIC part consists of the Maxwell and Lorentz solver and the particle treatment including movement, boundary conditions and localization. To test its functioning, electrons and protons are continuously injected into a square area from the left and the right side with a velocity of 10^3 m/s and 10^8 m/s, respectively.

Additionally, an external electric field of 10^6 V/m is applied in x-direction, thereby accelerating the par-

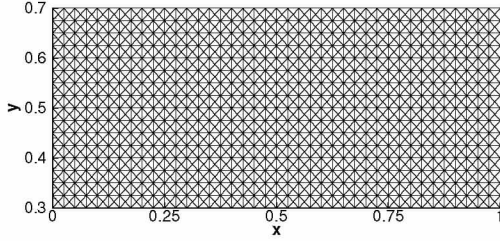


Figure 3: Grid used for the calculation of the verification test shown in Fig. 4.

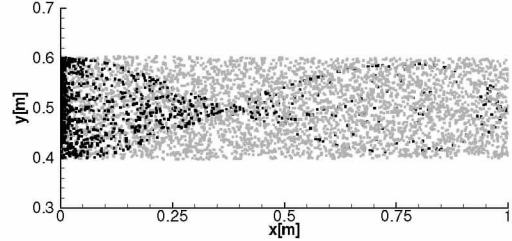


Figure 4: Particle distribution for a PIC verification test after 10 ns. Every 20th particle is displayed.

ticles. As can be seen in Fig. 4, the electrons (black) are accelerated towards the center of the proton (grey) “beam”. This behavior is expected due to the lower mass and therefore higher acceleration of the electrons. The cause for the striped appearance of the electrons is the interpolation, which – at the moment – assigns the same electric and magnetic field to all particles within a given grid cell.

In order to assess the applied model for (e,e)-collisions, we consider the situation where the distribution function of the scatterer is isotropic: $f(\vec{w}) = f(w)$, $w = |\vec{w}|$. Then, the Rosenbluth potentials only depend on the modulus of the speed, and may be computed by one-dimensional quadratures or the outlined Fourier approach, which is realized in the Rosenbluth solver. Explicitly, the resulting coefficients of friction $\mathcal{F}_f(c)$ and diffusion $D_{\perp}(c)$ and $D_{\parallel}(c)$ are analytically given.¹³ Transforming the FP equation (26) into spherical coordinates,⁸ one obtains the corresponding FP equation²⁰ for the distribution function $g(c, t) = c^2 f(c, t)$ of the isotropic case and from this the equivalent Langevin-type SDE

$$dc(t) = \left[\mathcal{F}_f(c) + \frac{D_{\perp}(c)}{c} \right] dt + \sqrt{D_{\parallel}(c)} dw(t) \quad (35)$$

for the scattered electrons, which is coded in the Langevin solver. Two numerical experiments based on the isotropic model are presented in the following.

Experiment 1: This numerical experiment is designed for the assessment of the applied approximation path and allows to identify possible insufficiencies as well as to suggest further improvements. It is well-known that one solution of the FP equation is the Maxwell distribution function¹³

$$g_0(c) = \frac{2}{\sqrt{2\pi} v_{th}^3} c^2 \exp\left\{-\frac{c^2}{2v_{th}^2}\right\}. \quad (36)$$

Initializing the numerical experiment according to the Maxwellian (36) with $v_{th} = 5$, we expect that the temporal evolution of the distribution function obtained from the simulation should stay very close to the Maxwellian shape. Fig. 5 shows the theoretical curve (full line) together with the solution (open squares) obtained with 256 velocity grid points after $2 \cdot 10^4$ iteration cycles. The numerical solution fits very well with the analytical one especially in the high-energy tail whose resolution is often critical because of the low number of particles. However, some fluctuations are observed around the maximum value of the distribution function. In order to analyze this observation, the time history of the mean (upper plot) and the variance (lower plot) is recorded in Fig. 6. These plots clearly reveal that the sample mean increase slightly with time while the variance decays. This behavior represents a typical fingerprint for a finite-sample noise-induced instability.²⁶ Especially, the noise-induced cooling (the variance decreases) is significant for systems which spend much time in equilibrium as in our case. A simple remedy to eliminate the fluctuations is the renormalization method introduced by Lemons and co-workers,²⁶ which will improve our proposed intraspecies collision approach.

Experiment 2: The initial data for this experiment are given by the isotropic, but non-Maxwellian velocity distribution

$$g_0(c) = \frac{1}{c_2 - c_1} \left[\Theta(c - c_1) - \Theta(c - c_2) \right]; \quad c_1 < c_2, \quad (37)$$

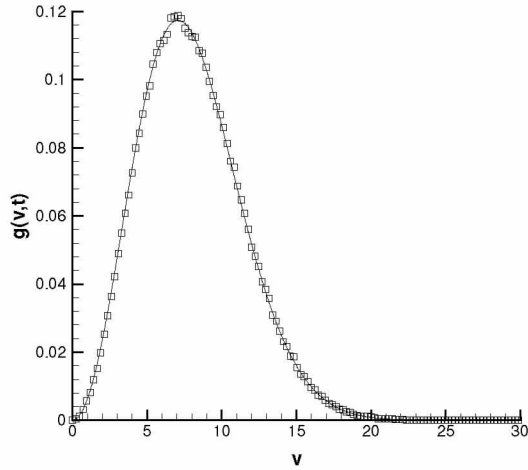


Figure 5: Comparison between the exact solution (full line) and the simulation result (open squares) after $2 \cdot 10^4$ cycles in time.

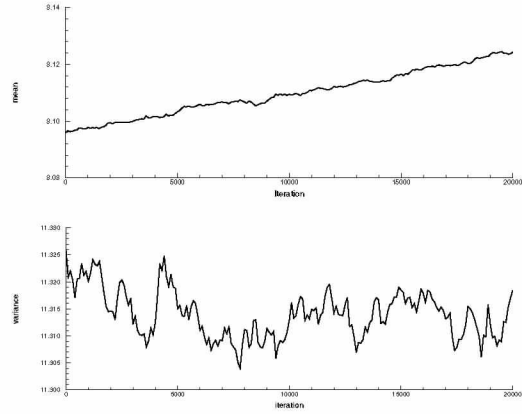


Figure 6: Time history of the sample mean value (upper) and variance (lower plot) for experiment 1.

where Θ is the Heaviside step function and $c_1 = 4$ and $c_2 = 5$. This profile (dashed line) is seen in Fig. 7 together with four further velocity distributions recorded at the (dimensionless) times $t = 1$ (full line), $t = 5$ (dashed-dotted line), $t = 10$ (line with squares) and $t = 40$ (line with circles). First, we observe a drastic change of the shape of the velocity distribution between $t = 0$ and $t = 5$. Afterwards, the change is less pronounced and a Maxwellian is discernible. At $t = 40$, the final Maxwellian distribution is reached, and further deviations from this shape are very small. Besides the shape of the distribution function, other quantities seemed to be helpful to study the collisional relaxation of a non-Maxwellian to a Maxwellian distribution. For this, the temporal evolution of the mean value (line with squares) and the variance (line with gradients) of the velocity distribution $g(c, t)$ as well as the quantity $H(t) = - \int dc \ln[g(c, t)] g(c, t)$ (line with circles) are presented in Fig. 8. Especially the latter quantity indicates that the obtained solution is close to the stationary solution, since only a small increase of $H(t)$ is observed in the long range time limit.

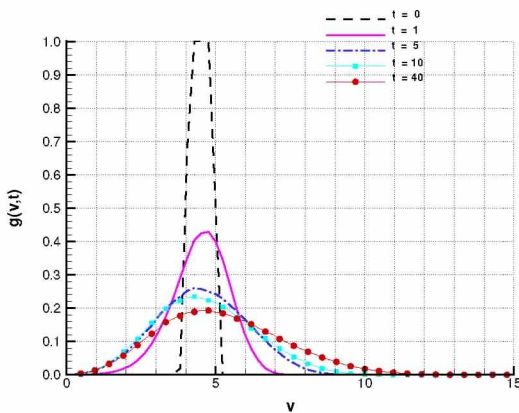


Figure 7: Temporal evolution of an initially isotropic but non-Maxwellian velocity distribution.

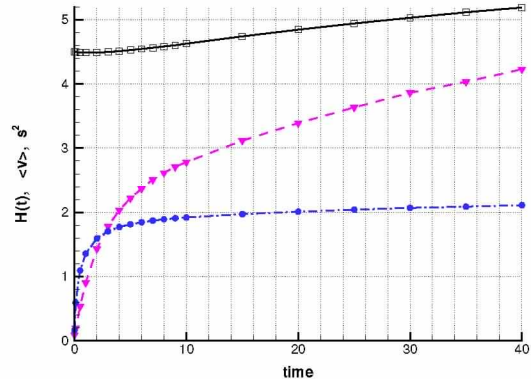


Figure 8: Mean value $\langle v \rangle$ (upper), variance σ^2 (middle) and $H(t)$ (lower curve) as a function of time for the velocity distribution $g(c, t)$.

VIII. Summary and Outlook

In cooperation between IRS, IAG, IHM and HLRS, a new numerical scheme is under development, intended to solve the Boltzmann equation for chemically reacting, non-continuum plasma flows, taking electromagnetic forces into account. In order to simulate instationary magnetoplasmadynamic thrusters and the CETEP system proposed by ESA, the requirements of three dimensional discretization and time accuracy complete the challenging task. Since a direct simulation of all atoms present in a macroscopic device like an electric propulsion system is far from being possible, statistical approaches are being used.

In order to simulate the coupling between electric and magnetic fields and charged particles, methods known from PIC schemes are used. The coupling between the charged particles itself has not been addressed in the context of PIC schemes so far. Therefore, a new model based on the Fokker-Planck equation is under development in order to describe intraspecies charged particle collisions. Inelastic collisions and short range interactions, i.e. collisions with neutral particles, leading to energy exchange, momentum exchange and to chemical reactions, are modeled using DSMC techniques.

Currently, the different models have been combined into one numerical code and verification testing of the different modeling approaches is in progress. Concurrently, data and operation structures are revised in order to allow for an efficient processing of the code on parallel vector high-performance computers.

Preliminary results of the verification tests have been shown. After successful completion of the verification tests of the different models, more sophisticated verification tests for the coupling of all modules are planned for the near future. Subsequent improvement of the modeling and optimization of most of the modules in order to improve vector performance and to reduce computational time will be ongoing.

IX. Acknowledgments

We gratefully acknowledge the Landesstiftung Baden-Württemberg for funding the present work. Torsten Stindl wishes to thank the State of Baden-Württemberg and the Erich-Becker-Stiftung, Germany, for their financial support.

References

- ¹Nawaz, A., Auweter-Kurtz, M., Herdrich, G., and Kurtz, H., "Investigation and Optimization of an Instationary MPD Thruster at IRS," International Electric Propulsion Conference, Princeton, USA, 2005.
- ²Nicolini, D. and Ockels, W., "Coupled Electrodynamical Tether/ Electrostatic Propulsion System," International Electric Propulsion Conference, Toulouse, France, 2003.
- ³Cosmo, M. and Lorenzini, E., "Tethers in Space Handbook," The Smithsonian Astrophysical Observatory, Cambridge, Third Edition, 1997.
- ⁴Munz, C.-D., Schneider, R., Sonnendrücker, E., Stein, E., Voß, U., and Westermann, T., "A Finite-Volume Particle-In-Cell Methode for the Numerical Treatment of the Maxwell-Lorentz Equations on Boundary-Fitted Meshes," *Int. J. Numer. Meth. Eng.*, Vol. 44, 1999, pp. 461–487.
- ⁵Munz, C.-D., Schneider, R., and Voß, U., "A Finite-Volume Particle-in-Cell Method for the Numerical Simulation of Devices in Pulsed Power Technology," *Surv. Math. Ind.*, 1999.
- ⁶Laux, M., *Direkte Simulation verdünnter, reagierender Strömungen*, Ph.D. thesis, Institut für Raumfahrtssysteme, Universität Stuttgart, Germany, 1996.
- ⁷Diver, D., *A Plasma Formulary for Physics, Technology, and Astrophysics*, Wiley-VCH Verlag, Berlin, 2001.
- ⁸Rosenbluth, M., MacDonald, W., and Judd, D., "Fokker-Planck Equation for an inverse-square Force," *Phys. Rev.*, Vol. 107, 1957, pp. 1–6.
- ⁹Fedoruk, M., Munz, C.-D., Omnes, P., and Schneider, R., "A Maxwell-Lorentz Solver for Self-Consistent Particle-Field Simulations on Unstructured Grids," Tech. Rep. FZKA 6115, FZKA, Karlsruhe, Germany, July 1998.
- ¹⁰Halter, E., Krauß, M., Munz, C.-D., Schneider, R., Stein, E., Voß, U., and Westermann, T., "A Concept for the Numerical Solution of the Maxwell-Vlasov System," Tech. Rep. FZKA 5654, FZKA, Karlsruhe, Germany, 1995.
- ¹¹Hockney, R. and Eastwood, J., *Computer Simulation using Particles*, McGraw-Hill, New York, 1981.
- ¹²Munz, C.-D., Omnes, P., and Schneide, R., "A three-dimensional finite-volume solver for the Maxwell equations with divergence cleaning on unstructured meshes," *Computer Physics Communications* 130 (2000) 83-117, 1999.
- ¹³Montgomery, D. and Tidman, D., *Plasma Kinetic Theory*, McGraw-Hill, New York, 1964.
- ¹⁴Nicholson, D., *Introduction to Plasma Theory*, Wiley, New York, 1983.
- ¹⁵Mitchner, M. and Krüger, C., *Partially Ionised Gas*, Wiley, New York, 1973.

- ¹⁶Gardner, C., *Handbook of Stochastic Methods*, Springer Verlag, Berlin, Heidelberg, New York, 1985.
- ¹⁷Honerkamp, J., *Stochastische Dynamische Systeme*, VCH Verlagsgesellschaft, Weinheim, 1990.
- ¹⁸Kloeden, P. and Platen, E., *Numerical Solution of Stochastic Differential Equations*, Springer-Verlag, Berlin, Heidelberg, New York, 1992.
- ¹⁹Manheim, W., Lampe, M., and Joyce, G., "Langevin Representation of Coulomb Collision in PIC Simulation," *Journal of Computational Physics*, Vol. 138, 1997, pp. 563–584.
- ²⁰Albright, B., Winske, D., Lemons, D., and Daughton, W. Jones, M., "Quite Simulation of Coulomb Collision," *IEEE Trans. Plasma Sci.*, Vol. 31, 2003, pp. 19–24.
- ²¹Hassani, S., *Mathematical Physics*, Springer, New York, Berlin, 1999.
- ²²Press, W. H., Flannery, B. P., Teukolsky, S. A., and Vetterling, W. T., *Numerical Recipes*, Cambridge University Press, Cambridge, 1987.
- ²³Brigham, E., *FFT; Schnelle Fourier-Transformation*, R. Oldenbourg Verlag, München, 1992.
- ²⁴Kloeden, P., Platen, E., and Schurz, H., *Numerical Solution of SDE Through Computer Experiments*, Springer-Verlag, Berlin, Heidelberg, New York, 2003.
- ²⁵Bird, G., *Molecular Gas Dynamics and the Direct Simulation of Gas Flows*, Clarendon Press, Oxford, 1994.
- ²⁶Lemons, D., Lackman, J., Jones, M., and Winske, D., "Noise-induced instability in self-consistent Monte Carlo calculations," *Physical Review E*, Vol. 52, 1995, pp. 6855–6861.